Ecological Modelling 222 (2011) 573–579

Contents lists available at ScienceDirect

Ecological Modelling

journal homepage: www.elsevier.com/locate/ecolmodel

Increasing accuracy of dispersal kernels in grid-based population models

D.H. Slone*

USGS Southeast Ecological Science Center, 2201 NW 40th Terrace, Gainesville, FL 32605, USA

ARTICLE INFO

Article history:
Received 19 January 2010
Received in revised form
20 November 2010
Accepted 23 November 2010
Available online 14 December 2010

Keywords:
Map lattice
Spatial model
Invasion model
Numerical simulation
Redistribution

ABSTRACT

Dispersal kernels in grid-based population models specify the proportion, distance and direction of movements within the model landscape. Spatial errors in dispersal kernels can have large compounding effects on model accuracy. Circular Gaussian and Laplacian dispersal kernels at a range of spatial resolutions were investigated, and methods for minimizing errors caused by the discretizing process were explored. Kernels of progressively smaller sizes relative to the landscape grid size were calculated using cell-integration and cell-center methods. These kernels were convolved repeatedly, and the final distribution was compared with a reference analytical solution. For large Gaussian kernels ($\sigma > 10$ cells), the total kernel error was $<10^{-11}$ compared to analytical results. Using an invasion model that tracked the time a population took to reach a defined goal, the discrete model results were comparable to the analytical reference. With Gaussian kernels that had $\sigma \leq 0.12$ using the cell integration method, or $\sigma \leq 0.22$ using the cell center method, the kernel error was greater than 10%, which resulted in invasion times that were orders of magnitude different than theoretical results. A goal-seeking routine was developed to adjust the kernels to minimize overall error. With this, corrections for small kernels were found that decreased overall kernel error to $<10^{-11}$ and invasion time error to <5%.

Published by Elsevier B.V.

1. Introduction

Spatially explicit population models are useful for forecasting spatial processes that cannot be solved with single-location analytical models. They combine temporal reproduction and mortality processes with spatial redistribution processes. The earliest spatial population models were analyzed with continuous time and space equations (e.g. Kolmogorov et al., 1937), and this form is still important and useful (e.g. Andow et al., 1990; Lutscher et al., 2007). Continuous systems allow for exact solutions to research questions such as density of organisms and speed of invasion wavefronts at a given time and place. They simulate populations that have free, or non-seasonal, reproduction throughout the time domain.

For modeling organisms that have a distinct breeding season, integro-difference models that are discrete in time, but continuous in space, are often used (e.g. Neubert and Caswell, 2000; Lutscher and Lewis, 2004). Because of increased complexity in the model system compared to all-continuous models, numeric fast-Fourier transformations or numerical solutions are commonly found in ecological applications of integro-difference dispersal models, rather than analytical solutions (e.g. Kot et al., 1996). Because of computational complexity, theoretical spatial processes are often developed first in continuous space, and then demonstrated with a grid-based discrete map lattice (e.g. Lutscher and Lewis, 2004).

1.1. Discrete-space models

If a continuous-space model is analytically intractable or if a fragmented, realistic map landscape is desired, the landscape of interest can be modeled directly in discrete space. Methods of discretizing space include nodal models that simulate the measured distances and directions among habitat nodes (spatially explicit population model; Dunning et al., 1995), or simulate the "movement cost" associated with movement between two nodes (Minor and Urban, 2007). These "graph models" are by definition unconcerned with the space between nodes of interest. Space can also be subdivided into grids that simulate all of the landscape of interest. Irregular grids, such as unstructured polygonal meshes or curvilinear grids, allow for different sized cells to concentrate computing power and resolution in those locations that are more complex. This approach has been used to model hydrodynamics (e.g. Bockelmann et al., 2004; Crowder and Diplas, 2000), but apparently not for animal or plant models due to the complexity of calculating dispersal in cells that have various sizes and spatial arrangements.

Subdividing the spatial domain into a map lattice of regular polygons (generally squares) simplifies dispersal modeling. Grid-based kernel redistribution models are useful for simulating spatial dispersal processes such as invasion in complex, natural landscapes with varying features and multiple types of irregular habitat

* Tel.: +1 352 264 3551; fax: +1 352 374 8080.
E-mail address: dslone@usgs.gov

0304-3800/$ – see front matter. Published by Elsevier B.V.
doi:10.1016/j.ecolmodel.2010.11.023

patches. Dispersal routines in grid-based population models specify the proportion, distance and direction of movement within each cell of the model landscape. Dispersal methods in regular grid models include global redistribution (e.g. King and Hastings, 2003), and nearest-neighbor redistribution (e.g. cellular automata; Ellner et al., 1998). A flexible modeling paradigm that can be applied to both graphs and (with effort) grids is circuit theory (McRae et al., 2008).

To simulate local dispersal processes in a grid-based spatial system, a continuous dispersal kernel, or probability density function for redistribution, can be split into component cells to generate and apply a discrete kernel through spatial convolution (Allen et al., 2001) or similarly, to apply a displacement matrix (Sebert-Cuvillier et al., 2008; Westerberg and Wennergren, 2003).

1.2. Problems with discrete spatial models

Standard terminology for cartographic standards, modified for ecological use, will be used (Dungan et al., 2002). "Spatial extent" is the overall size of the spatial domain, and "grain size" is the size of the cells in the landscape grid relative to the spatial extent. As the grain size decreases, the number of cells within a given spatial extent (the resolution) increases, and the accuracy of spatial processes, such as dispersal, increases.

Kernel smoothing and accuracy measures for "binned" data, and the determination of what grain size is needed for a given level of accuracy has been well documented (Jones, 1989; González-Manteiga et al., 1996; Hall and Wand, 1996; Pielaat et al., 2006). With classical numerical simulation of a complicated system that cannot be solved analytically, the grain of the landscape can be dynamically adjusted to preserve a defined, low error rate. For theoretical applications in discrete systems with a small spatial extent, a small grain size can be implemented for good accuracy. However, if the landscape is large compared to the dispersal abilities of the organism, a fine grain size for detailed dispersal kernels would lead to a very large number of cells across the spatial domain, thus requiring large amounts of computer processor power, RAM and data storage. Depending on the complexity of non-dispersal operations, the amount of time needed to run grid-based models tends to increase to the fourth power of the number of cells in any linear dimension of the simulation, so the time to run a simulation quickly increases as the spatial resolution becomes finer.

For some applications, the resolution of the model is already set due to precedent models or available data resolution (e.g. satellite imagery), and the modeler must work within that framework. For example, there are several spatial population models that support decision-making in the greater Everglades restoration process (CERP; http://www.evergladesplan.org/). Many of these models are driven by hydrological state variables, such as water depth or salinity. Hydrological models that provide these variables are available for different regions and purposes in 2×2 mile squares (SFWMM; SFWMD, 2005), 500×500 m (ATLSS; DeAngelis et al., 1998), or 400×400 m (EDEN; Liu et al., 2009). Land managers generally expect ecological model output to be in the same grid system as the hydrological models for consistency and ease of interpretation. These pre-defined grid sizes can lead to very coarse-grained spatial processes and small dispersal kernels. Climate models often are calculated with grid sizes of several kilometers. Downscaling to a finer scale presents substantial challenges and effort (Araújo et al., 2005), so tools to use coarse-scale models directly would be useful.

When dispersal of organisms is introduced to a discrete spatial model, the square shape of the landscape cells introduces errors in distance and direction as compared to the analytical dispersal process. Simple discrete dispersal methods such as nearest-neighbor, where propagules are redistributed only to the nearest contiguous cells, limit dispersal patterns, and are inappropriate for wide-ranging organisms. Using a discrete form of the continuous integro-difference redistribution kernel may reduce spatial errors compared to a simple nearest-neighbor distribution process, but each cell in the kernel can only contain one constant density, while a continuous dispersal kernel can change value over the same space. For some applications, a fine temporal scale may be desired. As the time step decreases, dispersal kernels become smaller and more coarse-grained. As the grain size is increased and the number of cells in a dispersal kernel shrinks, the information contained within the kernel also shrinks, and the kernel tails become less well defined. Very coarse kernels can essentially be reduced to a nearest-neighbor situation. These coarse kernels can be expected to contain large spatial errors (Hall and Wand, 1996; Fig. 1).

Errors that are generated by the discretization of spatial processes have always been tacitly acknowledged by researchers performing traditional numerical solutions to continuous spatial processes, so they use very fine grain sizes or error-controlling numerical methods (such as Runge-Kutta) in their simulations. Recently, uncontrolled error that appears in discrete model systems where the grain size is pre-selected and large is receiving attention in the literature (Chesson and Lee, 2005; Holland et al., 2007; O'Sullivan and Perry, 2009). Significant dispersal errors were found in a model described by Slone et al. (2003), caused by small size dispersal kernels on a large-grained landscape. For that model, the authors corrected the specific kernels used on an ad-hoc basis, but questions remained about the general error rates of small kernels. Measuring and correcting these errors will be the central focus of this paper.

2. Methods

2.1. Defining and correcting errors

Accurate dispersal kernels are necessary for spatial models to be reliable tools for answering management questions. As grain size decreases towards zero, results from a discrete simulation will asymptotically approach that of a continuous-space simulation (i.e. – have zero error). Two questions that arise are (1) at what grain size does the error between the discrete and continuous system become negligible for answering research questions, and (2) at coarser resolutions, can the error be corrected so that more efficient coarse-grained simulated landscapes can be used?

The research has the following three objectives:

1) quantify error in discrete Gaussian and Laplace dispersal kernels, and the invasion speed of these kernels when applied to a spatial model;
2) explore methods to correct kernel error, thus allowing the output from coarse-grained discrete spatial systems to match theoretical or field-measured dispersal rates; and
3) determine a minimum grain size where no correction is required (<5% error in invasion speed).

Though population redistribution functions are often non-normal (Kot et al., 1996), the bivariate Gaussian distribution was explored first because it exhibits "closure" (Chesson and Lee, 2005): that is, as organisms disperse from a single cell through time with a Gaussian dispersal kernel, their overall distribution will remain Gaussian, with known parameters. This property enables a simple but powerful test: as a Gaussian dispersal kernel becomes very small, do the propagules still disperse in the expected pattern and retain the expected Gaussian distribution? Other kernel shapes do not lend themselves so readily to this type of analysis. The Gaussian kernel – assuming non-directional circular dispersal ($\mu_x = \mu_y = 0$; $\sigma_x = \sigma_y = \sigma$) – has an additional simplifying property that it has only one parameter (σ; see Table 1 for notation).

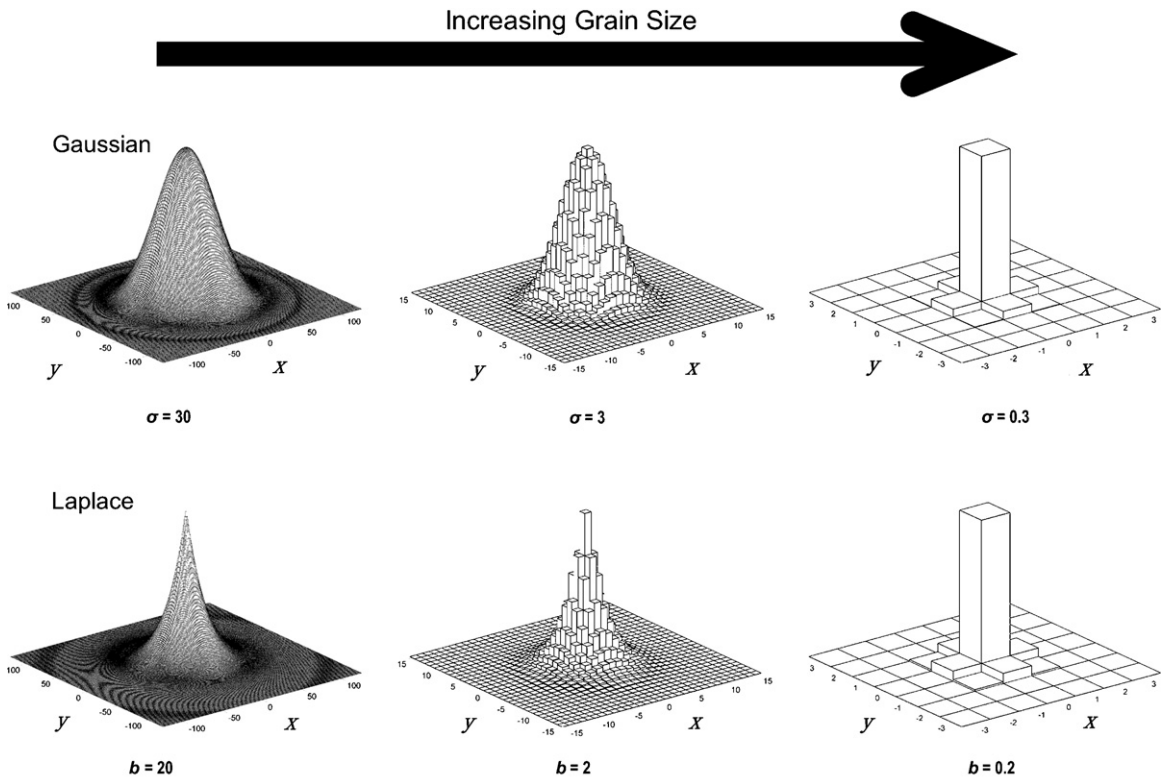

Fig. 1. Dispersal kernels of different standard deviations: smaller kernels are more spatially inaccurate, and also converge to a common shape (only the center portions of the larger distributions are displayed).

For kernels that do not exhibit closure, a practical dispersal test can be conducted to ascertain whether speed of invasion remains consistent over a fixed distance as the grain size of the simulation changes. The circular Laplace (exponential decay) kernel and also the Gaussian kernel were tested in this way.

2.2. Dispersal kernel functions

Dispersal in continuous space integro-difference models is accomplished through use of a spatial convolution model of the form:

$$N_t(i, j) = \iint_{x,y} k(x, y) f(N_{t-1}(i-x, j-y))\, dx\, dy, \tag{1}$$

(Kot et al., 1996; Lutscher and Lewis, 2004), where $k(x,y)$ represents the dispersal kernel for the species in question, and $f(N_{t-1}(i,j))$ is some function that transfers the population from one time step to the next. The dispersal kernel k can be any probability density function (pdf). For grid-based discrete ecological models (Allen et al., 2001), the continuous convolution process above becomes the analogous discrete convolution:

$$N_t(i, j) = \sum_x \sum_y k(x, y) f(N_{t-1}(i-x, j-y)). \tag{2}$$

This equation may be solved by multiplying the 2-d fast Fourier transforms of k and f together and then inverting in a time loop to visualize the spatial dynamics, and when k is large relative to the spatial domain, this may be computationally efficient. In practice, however, most ecologists are simulating very large spatial domains relative to the dispersal of their organisms, implying that k is very small relative to the spatial extent of f. In this case, the direct convolution is usually faster.

Two methods were compared for calculating discrete kernels. For the first method, the value of the appropriate continuous distribution was calculated at the center of each cell of the array, and used as the value for that cell (center method):

$$k_{[x,y]} = \frac{1}{2\pi\sigma^2} \exp\left(-\frac{x^2+y^2}{2\sigma^2}\right), \tag{3}$$

where σ is measured in grid cell units.

For the second method, which was more computationally intensive but more indicative of the actual density of organisms moving to each cell, the part of the continuous probability distribution that fell within each cell was integrated. The resulting value was used as the value of that cell (integrated method):

$$k_{[x,y]} = \int_{x-0.5}^{x+0.5} \int_{y-0.5}^{y+0.5} \frac{1}{2\pi\sigma^2} \exp\left(-\frac{x^2+y^2}{2\sigma^2}\right). \tag{4}$$

Table 1
Notation.

Variable	Definition
k	Distribution kernel function
x, y	Spatial coordinates of distribution kernel
N	Population density at each location
i, j	Spatial coordinates of model landscape
t	Time step of model
f	Population reproduction or mortality function
μ	Mean of the Gaussian kernel
σ	Standard deviation (spread) of the Gaussian kernel
σ'	Corrected standard deviation of the Gaussian kernel
b	Scale (spread) of the Laplace distribution
b'	Corrected scale of Laplace distribution
n	Number of convolutions applied
$*$	Spatial convolution operator

Most testing was performed using these two variations of the Gaussian kernel. Additional invasion speed tests were performed using the center-calculated circular Laplace distribution. It also has only one parameter (b), which is analogous to the σ parameter of the Gaussian distribution:

$$k_{[x,y]} = \frac{1}{b} \cdot \exp\left(-\frac{1}{b}\sqrt{x^2+y^2}\right). \quad (5)$$

The spatial extent of each kernel was set to $12\sigma+1$ cells for the Gaussian kernels and $12b+1$ cells for the Laplace kernels, with a minimum of 5×5 cells. For example, a Gaussian kernel with σ of 10 was 121×121 cells, while a Gaussian kernel with σ of 0.1 was 5×5 cells, because $12(0.1)+1 = 2.2$. This rule generated kernels that had densities of less than 10^{-16} at their periphery. All kernels were normalized by dividing each cell of the kernel by its sum:

$$k^*_{[x,y]} = \frac{k_{[x,y]}}{\sum_x \sum_y k}, \quad (6)$$

thus assuring that each kernel summed to 1 and maintained a constant population abundance as it was applied.

2.3. Quantifying discrete dispersal kernel error

A Gaussian kernel exhibits "closure" (Chesson and Lee, 2005), such that a kernel $k(\sigma, x, y)$ that is convolved n times (repeated dispersal events) is theoretically equivalent to a single convolution of a large Gaussian dispersal kernel of size $k(\sigma\sqrt{n}, x, y)$:

$$k(\sigma, x, y)_1 * k(\sigma, x, y)_2 * \cdots * k(\sigma, x, y)_n * N(x, y) = k(\sigma\sqrt{n}, x, y) * N(x, y), \quad (7)$$

where * is the convolution operator. To measure the shape error of dispersal kernels, 2-D discrete convolution was applied repeatedly to a simulated population of size 10,000 placed in the center cell of a large discrete arena. The resulting distribution was then compared to the theoretical result.

As kernel size approaches infinity (i.e., grain size shrinks towards zero), the error induced by the "pixelation" of the discrete landscape also approaches zero. So, we might expect a large discrete dispersal kernel to show high fidelity to its theoretical parameters, while a smaller one would show less fidelity (Fig. 1). Through preliminary testing, a Gaussian kernel with a σ of 24 was found to contain negligible spatial error. To test the effect of size on spatial error, Gaussian kernels (k_{small}) with $0.01 \le \sigma \le 4$, were convolved $(24/\sigma)^2$ times, so the resulting distribution (k_{conv}) could be compared to a Gaussian kernel of $\sigma = 24$ (k_{large}). Larger Gaussian kernels with $4 \le \sigma \le 24$ were convolved 36 times and then compared to a k_{large} kernel with $\sigma_{large} = 6\sigma_{small}$. This methodology was repeated for each of the two kernel generation methods (center and integrated), with k_{large} and k_{small} being generated with the same method. There was no simulation of immigration, emigration, reproduction or mortality, so the total population size in all simulations remained constant.

To measure error in the k_{conv} kernels, the pairwise sum-of-squares error (SSE) was calculated for the entire spatial domain:

$$SSE = \sum_x \sum_y \left[k_{conv}(x, y) - k_{large}(x, y)\right]^2. \quad (8)$$

2.4. Correcting dispersal kernel error

For each dispersal kernel of size σ, there was an associated n, or the number of convolutions used to generate the uncorrected k_{large}. An adaptive gradient descent algorithm was used to test new values of σ for each value of n, to minimize the SSE between k_{conv} and k_{large}. This procedure ultimately resulted in a corrected value for each σ, called σ'.

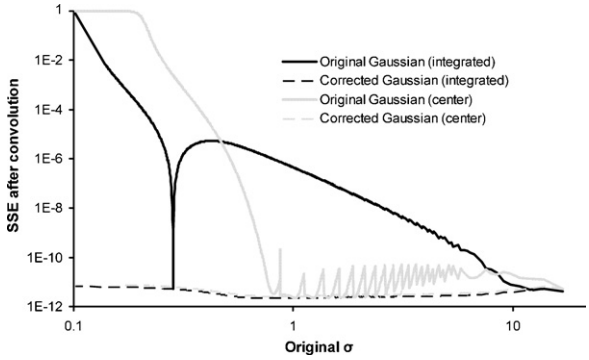

Fig. 2. Spatial error was measured after repeated convolution of Gaussian dispersal kernels of a single population placed in the center cell, with smaller kernels showing dramatic errors in population distribution. Integrated = kernel calculated using integrated method; center = kernel calculated using center method.

Finally, a simple invasion scenario was developed to test the speed of invasion of the uncorrected and corrected values of σ. For each value of σ, a square grid map was created with a size that was the larger of either $100\sigma+1$, or 41 cells. In the center cell of this map, a population of 10,000 individuals was added, and then the uncorrected Gaussian kernel was convolved with the map until a cell at the edge of the map had a population > 1. This number of convolutions was recorded. Next, the respective corrected kernels were convolved with the same scenario, and the number of convolutions needed for the population to reach the edge of the map was recorded.

To assess whether a dispersal kernel could be corrected without resorting to analysis of the kernel size and shape, an adaptive gradient descent algorithm was used to directly optimize σ by matching the number of time steps the discrete invasion model took to reach the edge to the theoretical number of time steps that an equivalent continuous model took. After several values of σ were corrected, a polynomial regression was fitted to $\ln(\sigma'/\sigma)$, and then this regression was tested using the full range of σ values in the invasion model, again by comparing the number of time steps the discrete model took relative to the continuous model.

Finally, a similar invasion scenario was run using the Laplace distribution. Again using a gradient descent goal-seeking algorithm, the invasion model was processed for several levels of b until optimum corrected values (b') were found that matched the expected continuous-space results. A polynomial regression was fitted to $\ln(b'/b)$, and this equation was validated by choosing a wide range of values of b' to compare with the continuous-space results.

Analysis was performed in Matlab, 2007a (The Mathworks, Inc., Natick, MA, USA) with double-precision floating point calculations.

3. Results and discussion

3.1. Quantifying discrete dispersal kernel error

Dispersal error increased rapidly in both center and integrated methods for $\sigma > 1$ (Fig. 2). Whereas the center method produced a somewhat better fit than the integrated method for medium-sized kernels (σ from 0.45 to 7.5), it produced much larger errors for small kernels below $\sigma = 0.45$. For simulation models with low resolution, uncorrected kernels generated with the center method would generally show slower invasion speed than the corresponding analytical result. This pattern has been seen in the literature where the analytical and numerical results were plotted together (e.g. Fig. 5 in Kot et al., 1996; Figs. 1 and 2 in Méndez et al., 2002). Numerical simulations with small kernels generated with the integrated method might show slower or faster invasion wavefronts,

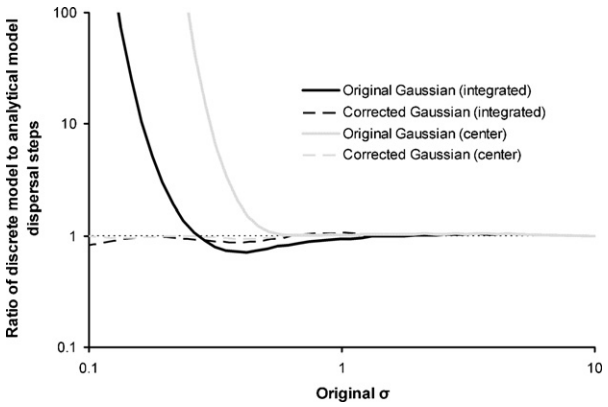

Fig. 3. Results of invasion test with Gaussian dispersal kernels generated by the integrated method (black lines) and by the center method (gray lines). Corrected kernels were derived from polynomial Eqs. (9) and (10) that were fitted to the curves plotted in this figure. Small residual errors in the corrected kernels were the result of error in the polynomial equation to the optimized kernels – optimizing each size of kernel directly would lead to an accurate invasion model for every size.

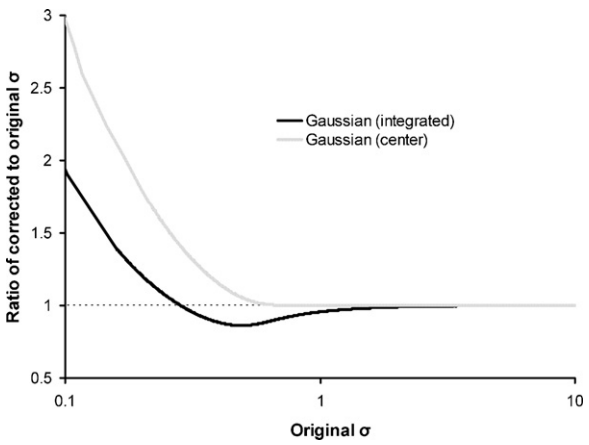

Fig. 4. The corrected kernels were generally larger than the uncorrected kernels – that is, if uncorrected, dispersal would be underestimated. Dispersal kernels with standard deviations that were smaller than 1 required more correction, with the center method requiring the most correction. Integrated = kernel calculated using integrated method; center = kernel calculated using center method.

depending on the resolution of the kernel and the precise ratio of the dispersal kernel to the map cell size.

3.2. Correcting dispersal kernel error

The invasion test confirmed that the error increased rapidly in small kernels. Accurate results were obtained without correction from the integrated method down to $\sigma = 2$ (Fig. 3), and with the center method down to $\sigma = 0.8$ (Fig. 3). Reasonable accuracy (within 10% error) was retained down to $\sigma = 0.3$ for the integrated method and $\sigma = 0.5$ for the center method, but below those values, accuracy degraded rapidly with decreasing standard deviation values.

For each method and each σ, a corrected kernel size (σ') was found that brought the total SSE to very small levels (<1e-11, Fig. 2), and also produced accurate invasion speed results (Fig. 3). As the size of σ decreased, the magnitude of correction necessary to minimize the total SSE increased (Fig. 4). The center method generally required a larger correction, especially for very small kernels. Regressions from the invasion model optimization were calculated

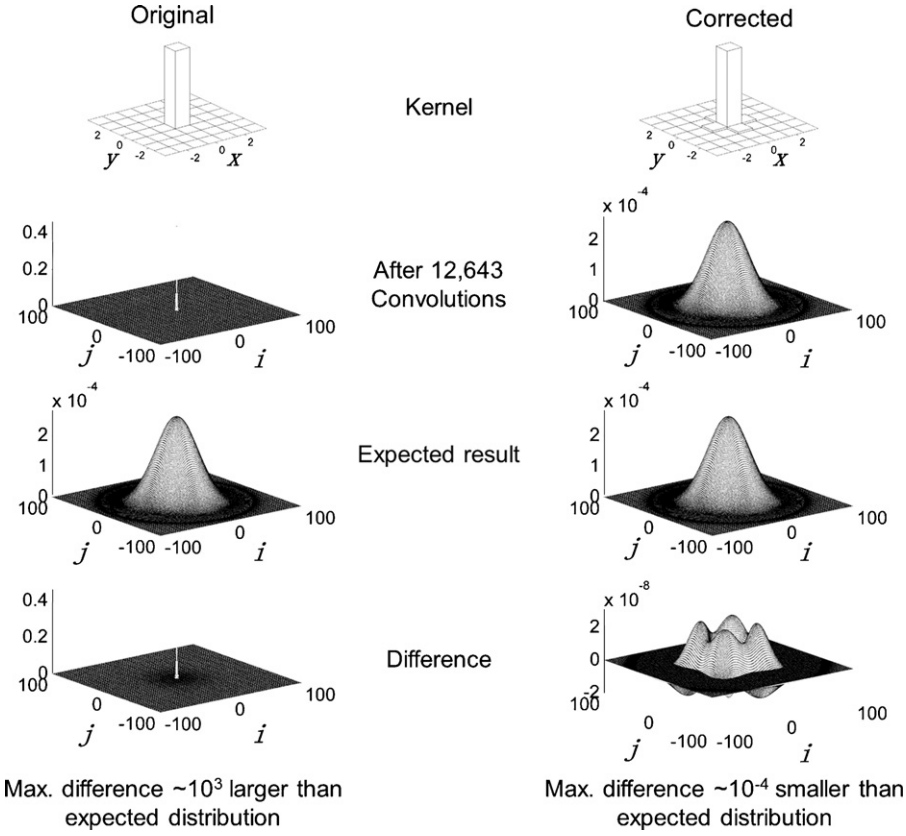

Fig. 5. An arbitrarily-chosen small Gaussian kernel using the Center calculation method and σ of 0.2134. The original uncorrected kernel is shown on the left, and the corrected kernel is on the right (only the center portions of the larger distributions are displayed). The correction reduced the population density error by approximately 8 orders of magnitude. Other sizes show similar results. Note that the scales may differ in each graph.

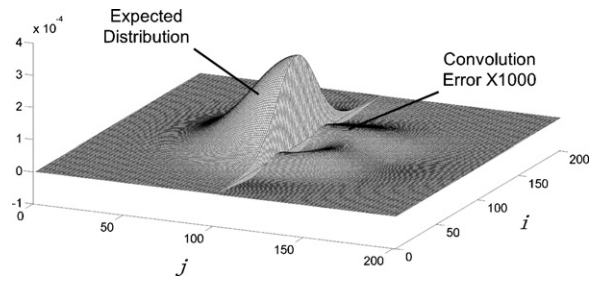

Fig. 6. Comparing the expected distribution (left) with the difference in the corrected kernel after convolution 12643 times. The error distribution was multiplied 1000× to make it visible (right). Near the center of the distribution, the error after convolution was more than 4 orders of magnitude (10^{-4}) smaller than the distribution, and near the periphery, the error was approximately 10^{-3} times the distribution. Only the center portions of the distributions are shown.

as follows. For integrated kernels with $\sigma < 2$:

$$\sigma' = \sigma \cdot (-0.1014 \cdot \ln(\sigma)^3 + 0.0097 \cdot \ln(\sigma)^2 + 0.1244 \cdot \ln(\sigma) + 0.9375), \quad (9)$$

and for center-calculated kernels with $\sigma < 0.8$:

$$\sigma' = \sigma.(0.0929.\ln(\sigma)^3 + 0.2226.\ln(\sigma)^2 + 0.1184.\ln(\sigma) + 1). \quad (10)$$

These equations reduced the error of invasion speed to <5% for $\sigma > 0.1$ (Fig. 3).

To visually demonstrate the dramatic difference in dispersal error before and after kernel correction, an arbitrary, small value of σ was chosen ($\sigma = 0.2134$, or 12,643 convolutions to generate a distribution $\sim N[0, 24]$) (Fig. 5). Before correction, the population starting from the center cell did not disperse more than a few cells from the center after 12,643 convolutions, indicating that the calculated kernel was effectively too small. Any application of this uncorrected kernel would lead to gross underdispersal of the modeled organism, compared to the analytical model solution. After correction, which only slightly increased the size of the kernel, the resulting population distribution was very close to the expected distribution. The error in the overall distribution on a cell-by-cell basis was generally less than 10^{-4} times the population density near the center of the distribution, and approximately 10^{-3} times the population density near the critical edges (Fig. 6). This level of error would be negligible compared to errors in other model processes.

While so far only the Gaussian kernel shape has been discussed, any kernel can be adjusted by performing a continuous-space analysis to obtain the theoretical number of time steps for an invading population to disperse to a distant cell, then adjusting the size parameter in the discrete domain until the number of time steps in the discrete model matches the theoretical result. This procedure could be used to calibrate any form of small discrete dispersal kernel, allowing for more biologically realistic leptokurtic shapes. Following this procedure, several center-calculated circular Laplace kernels of sizes $b = 0.01$ to $b = 1$were corrected, then a polynomial equation was fit to the points, and a general equation to correct an arbitrary sized Laplace kernel was generated:

For $b < 1.5$:

$$b' = b \cdot (-0.06 \cdot \ln(b)^3 - 0.0732 \cdot \ln(b)^2 + 0.077 \cdot \ln(b) + 0.9906). \quad (11)$$

This equation reduced invasion speed error to less than 2% for Laplace kernels with $b > 0.03$ (Fig. 7).

The invasion model method of correcting cannot guarantee that the total SSE of a corrected kernel would be vanishingly small. Given that the SSE for the Gaussian kernel was very small after correction for size, and this in turn also corrected for invasion speed, it may be reasonable to assume that SSE for the Laplace or other kernel shapes would also be small after correction for invasion speed.

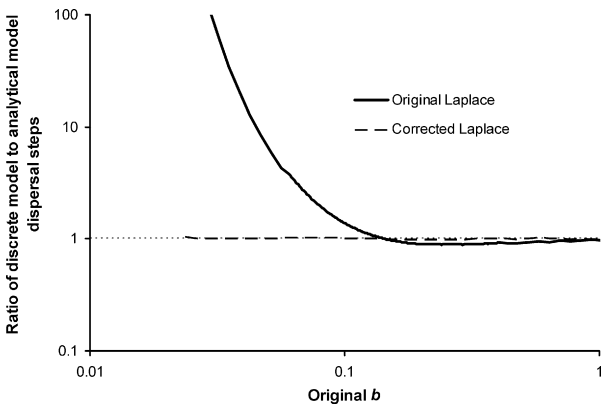

Fig. 7. Results of invasion test with Laplace kernels generated by the center method. Corrected kernel was generated by polynomial Eq. (11). As with the Gaussian kernel, the small, original Laplace kernels generally led to underestimation of dispersal, requiring too many dispersal steps to reach the goal. Correcting the kernels with Eq. (11) dramatically reduced that error.

4. Conclusions

This work demonstrates the danger inherent in using coarse-grained dispersal kernels in discrete spatial models. As discrete dispersal kernels are made smaller in size, the spatial error inherent in the kernel increases. This error propagates through repeated dispersal cycles until the population distribution looks nothing like its expected distribution. These errors can produce serious problems in interpretation if the model is to be used to predict real-world events, such as the time an invading population will take to reach a certain location. Correction of small kernels is required to make output from the discrete model equivalent to theoretical predictions. Correction of the width (σ for Gaussian, b for Laplace) of the kernel may be sufficient to fix the overall spatial error of dispersion, so discrete dispersal kernels can thus give accurate results, even when they are very small.

Exhaustive tests of kernel shapes other than Gaussian and Laplace were not performed because of the large number of possible kernel shapes (Chesson and Lee, 2005). If multiple convolutions of the kernel cannot be analyzed directly, then correcting the kernel based on an invasion test with a known expected result is possible. The polynomial correction equations (Eqs. (9)–(11)) were developed to correct for any arbitrary Gaussian or Laplace kernel, but this step would not be necessary for single dispersal kernels. In this case, only a single comparison and correction with the comparable analytical model would be required. Recent papers (e.g. Lindström et al., 2008; Sebert-Cuvillier et al., 2008) that focused on discrete invasion models demonstrate the research applicability of testing dispersal kernels for dispersal bias or lack thereof with an invasion model. Explicit testing for movement bias in models has been called for recently (Holland et al., 2007) due to demonstrated errors from individual-based movements in coarse-grained regular lattices. The results shown here that demonstrate significant errors from kernel-based movements in similar lattices also indicate the need for such testing.

If small spatial error is desired without correction, a conservative rule of thumb that has consistently worked for the author is that the kernel be large enough that at least half of the dispersing population of each cell leaves the cell during each convolution. With the Gaussian kernel this occurred with $\sigma > 0.56$ and with Laplace kernel this occurred with $b > 0.33$. It appears that kernels with fatter tails (e.g. Laplace) are less susceptible to error as the kernel shrinks, because more propagules are moved farther away from the center cell, and these far-flung propagules continue to provide mass to the

outer edges of the kernel, even when most of the mass remains in the center cell.

For discrete spatial models, the best mix of spatial and temporal accuracy, combined with speed of execution, may involve a large spatial domain and a small kernel that will be iterated several times during a simulation. A larger, more inherently accurate kernel may not be an optimum choice, because it would require fewer time steps to reach the goal, and so become temporally imprecise (large jumps in time between iterations). The spatial inaccuracy of small kernels can be overcome through the correction techniques presented here, making temporally fine spatial models more accurate and useful as management tools for real-world problems.

Acknowledgements

I thank two USGS reviewers and two journal reviewers for their helpful comments. Use of trade, product, or firm names does not imply endorsement by the U.S. Government.

References

Allen, J.C., Brewster, C.C., Slone, D.H., 2001. Spatially explicit ecological models: a spatial convolution approach. Chaos Solitons and Fractals 12, 333–347.
Andow, D.A., Kareiva, P.M., Levin, S.A., Okubo, A., 1990. Spread of invading organisms. Landscape Ecology 4, 177–188.
Araújo, M.B., Thuiller, W., Williams, P.H., Reginster, I., 2005. Downscaling European species atlas distributions to a finer resolution: implications for conservation planning. Global Ecology and Biogeography 14, 17–30.
Bockelmann, B., Fenrich, E., Lin, B., Falconer, R., 2004. Development of an ecohydraulics model for stream and river restoration. Ecological Engineering 22, 227–235.
Chesson, P., Lee, C.T., 2005. Families of discrete kernels for modeling dispersal. Theoretical Population Biology 67, 241–256.
Crowder, D., Diplas, P., 2000. Using two-dimensional hydrodynamic models at scales of ecological importance. Journal of Hydrology 230, 172–191.
DeAngelis, D., Gross, L., Huston, M., Wolff, W., Fleming, D., Comiskey, E., Sylvester, S., 1998. Landscape modeling for Everglades ecosystem restoration. Ecosystems 1, 64–75.
Dungan, J.L., Perry, J.N., Dale, M.R.T., Legendre, P., Citron-Pousty, S., Fortin, M.J., Jakomulska, A., Miriti, M., Rosenberg, M.S., 2002. A balanced view of scale in spatial statistical analysis. Ecography 25, 626–640.
Dunning Jr., J.B., Stewart, D.J., Danielson, B.J., Noon, B.R., Root, T.L., Lamberson, R.H., Stevens, E.E., 1995. Spatially explicit population models: current forms and future uses. Ecological Applications 5, 3–11.
Ellner, S.P., Sasaki, A., Haraguchi, Y., Matsuda, H., 1998. Speed of invasion in lattice population models: pair-edge approximation. Journal of Mathematical Biology 36, 469–484.
González-Manteiga, W., Sánchez-Sellero, C., Wand, M.P., 1996. Accuracy of binned kernel functional approximations. Computational Statistics and Data Analysis 22, 1–16.
Hall, P., Wand, M.P., 1996. On the accuracy of binned kernel density estimators. Journal of Multivariate Analysis 56, 165–184.
Holland, E.P., Aegerter, J.N., Dytham, C., Smith, G.C., 2007. Landscape as a model: the importance of geometry. PLoS Computers in Biology 3, 1979–1992.
Jones, M.C., 1989. Discretized and interpolated kernel density estimates. Journal of the American Statistical Association 84, 733–741.
King, A., Hastings, A., 2003. Spatial mechanisms for coexistence of species sharing a common natural enemy. Theoretical Population Biology 64, 431–438.
Kolmogorov, A.N., Petrovskii, I.G., Piskunov, N.S., 1937. Étude de l'équation de la diffusion avec croissance de la quantité de matière et son application à un problème biologique. Moscow University Bull. Math 1, 1–25.
Kot, M., Lewis, M.A., van den Driessche, P., 1996. Dispersal data and the spread of 470 invading organisms. Ecology 77, 2027–2042.
Lindström, T., Häkansson, N., Westerberg, L., Wennergren, U., 2008. Splitting the tail of the displacement kernel shows the unimportance of kurtosis. Ecology 89, 1784–1790.
Liu, Z., Volin, J., Dianne Owen, V., Pearlstine, L., Allen, J., Mazzotti, F., Higer, A., 2009. Validation and ecosystem applications of the EDEN water-surface model for the Florida Everglades. Ecohydrology 2, 182–194.
Lutscher, F., Lewis, M.A., 2004. Spatially explicit matrix models: a mathematical analysis of stage-structured integrodifference equations. Journal of Mathematical Biology 48, 293–324.
Lutscher, F., McCauley, E., Lewis, M., 2007. Spatial patterns and coexistence mechanisms in systems with unidirectional flow. Theoretical Population Biology 71, 267–277.
McRae, B., Dickson, B., Keitt, T., Shah, V., 2008. Using circuit theory to model connectivity in ecology, evolution, and conservation. Ecology 89, 2712–2724.
Méndez, V., Pujol, T., Fort, J., 2002. Dispersal probability distributions and the wavefront speed problem. Physical Review E: Statistical, Nonlinear, and Soft Matter Physics 65, 1–6.
Minor, E., Urban, D., 2007. Graph theory as a proxy for spatially explicit population models in conservation planning. Ecological Applications 17, 1771–1782.
Neubert, M., Caswell, H., 2000. Demography and dispersal: calculation and sensitivity analysis of invasion speed for structured populations. Ecology 81, 1613–1628.
O'Sullivan, D., Perry, G., 2009. A discrete space model for continuous space dispersal processes. Ecological Informatics 4, 57–68.
Pielaat, A., Lewis, M., Lele, S., De-Camino-Beck, T., 2006. Sequential sampling designs for catching the tail of dispersal kernels. Ecological Modelling 190, 205–222.
Sebert-Cuvillier, E., Simon-Goyheneche, V., Paccaut, F., Chabrerie, O., Goubet, O., Decocq, G., 2008. Spatial spread of an alien tree species in a heterogeneous forest landscape: a spatially realistic simulation model. Landscape Ecology 23, 787–801.
Slone, D.H., Rice, K.G., Allen, J., 2003. Model evaluates influence of Everglades restoration on alligator populations (Florida). Ecological Restoration 21, 141–142.
South Florida Water Management District (SFWMD), 2005. Final Documentation for the South Florida Water Management Model. Hydrologic & Environmental Systems Modeling Department, Everglades Restoration, SFWMD, West Palm Beach, Florida.
Westerberg, L., Wennergren, U., 2003. Predicting the spatial distribution of a population in a heterogeneous landscape. Ecological Modelling 166, 53–65.

Daniel H. Slone is a research ecologist at the USGS Southeastern Ecological Science Center. He works with population and habitat data analyses and simulation models, generally with West Indian manatees, Florida crocodilians, and seagrasses.